Electric polarization induced by a proper helical magnetic ordering in a delafossite multiferroic $CuFe_{1-x}Al_xO_2$

T. Nakajima,* S. Mitsuda, S. Kanetsuki, K. Tanaka, and K. Fujii
Department of Physics, Faculty of Science, Tokyo University of Science, Tokyo 162-8601, Japan

N. Terada
ICYS, National Institute for Materials Science, Ibaraki 305-0044, Japan

M. Soda, M. Matsuura, and K. Hirota
Institute for Solid State Physics, University of Tokyo, Kashiwa 277-8581, Japan
(Received 10 December 2007; published 4 February 2008)

We have established the relationship between the electric polarization vector and the local spin arrangement including vector spin chirality in delafossite multiferroic $CuFe_{1-x}Al_xO_2$. The results of polarized neutron diffraction and pyroelectric measurements demonstrate that proper helical magnetic ordering in $CuFe_{1-x}Al_xO_2$ induces a spontaneous electric polarization parallel to the vector spin chirality. This result cannot be explained by the Katsura-Nagaosa-Balatsky model, which successfully explains the ferroelectricity in recently explored ferroelectric helimagnets, such as $TbMnO_3$. We thus conclude that $CuFe_{1-x}Al_xO_2$ is another type of multiferroic.

DOI: 10.1103/PhysRevB.77.052401 PACS number(s): 75.80.+q, 75.25.+z, 77.80.−e

Novel types of couplings between dielectric properties and magnetism, which produce colossal magnetoelectric (ME) effects, have been extensively investigated since a gigantic ME effect was discovered in $RMnO_3$ (where R is a rare earth material).[1] Among several types of couplings between spin and electric polarization, ferroelectricity induced by a noncollinear spin arrangement has been most widely investigated experimentally and theoretically.[2–8] Katsura *et al.* proposed that the local electric dipole moment $\boldsymbol{p}$, which arises between two neighboring spins $\boldsymbol{S}_i$ and $\boldsymbol{S}_{i+1}$, can be described in the form of $\boldsymbol{p} \propto \boldsymbol{e}_{i,i+1} \times (\boldsymbol{S}_i \times \boldsymbol{S}_{i+1})$, where $\boldsymbol{e}_{i,i+1}$ is a unit vector connecting two spins.[2] This formula successfully explains the ferroelectricity of cycloidal or conical magnetic orderings of certain transition metal oxides, such as $RMnO_3$ (R=Tb,$Tb_{1-x}Dy_x$), $Ni_3V_2O_8$, $MnWO_4$, and $CoCr_2O_4$.[4–8] Moreover, a recent polarized neutron diffraction study on $TbMnO_3$ demonstrated that the spin helicity, clockwise or counterclockwise, correlates with the direction of the electric polarization, as predicted by the formula.[9] However, it has been recently reported that the ferroelectricity in several noncollinear magnets cannot be explained by the above formula,[10] for example, delafossite multiferroic $CuFeO_2$.[11] Therefore, $CuFeO_2$ provides an opportunity to explore another type of exotic spin-polarization coupling.

$CuFeO_2$, which is one of the model materials of a triangular lattice antiferromagnet, has been extensively investigated as a geometrically frustrated spin system for the last 15 years.[12–14] In the past several years, $CuFeO_2$ has been the subject of intense interest as a multiferroic material because of the discovery of spontaneous electric polarization, which emerges along the direction perpendicular to the hexagonal c axis, in the first field-induced phase.[15] Recent studies on the slightly diluted system $CuFe_{1-x}Al_xO_2$ showed that only a few percent dilution of magnetic Fe^{3+} sites with nonmagnetic Al^{3+} ions considerably reduces the transition field from the ground state, in which a collinear commensurate magnetic ordering is realized, to the ferroelectric phase. Moreover, the ferroelectric phase shows up even under zero field in the concentration region of $0.014 < x < 0.030$.[16–18] Quite recently, the magnetic structure in the ferroelectric phase was elucidated to be an antiferromagnetically stacked proper helical structure with a modulation wave vector $\left(q, q, \frac{3}{2}\right)$, where $q \sim 0.21$.[11] In this Brief Report, we refer to this ferroelectric phase as the ferroelectric incommensurate (FEIC) phase. This magnetic structure cannot lead to a finite uniform electric polarization through the formula $\boldsymbol{p} \propto \boldsymbol{e}_{i,i+1} \times (\boldsymbol{S}_i \times \boldsymbol{S}_{i+1})$ because the direction of $\boldsymbol{e}_{i,i+1}$ is parallel to the direction of $\boldsymbol{S}_i \times \boldsymbol{S}_{i+1}$ on average. We thus anticipate that another type of spin-polarization coupling is realized in $CuFe_{1-x}Al_xO_2$. To discuss the microscopic mechanism of the spin-polarization coupling in this system, it is critical to establish the relationship between the electric polarization vector and the magnetic modulation wave vector. In this Brief Report, we present polarized neutron diffraction and pyroelectric measurements on $CuFe_{1-x}Al_xO_2$ with x=0.02, revealing the relationship, which has not been elucidated by previous (bulk) dielectric measurements owing to the existence of three magnetic domains reflecting the threefold symmetry of the crystal structure.[15,17] We have found that the local electric polarization vector in $CuFe_{1-x}Al_xO_2$ arises along the helical axis of the proper helical magnetic ordering, and there is a one-to-one correspondence between the directions of the polarization vector and the spin helicity, a right-handed- (RH) or left-handed- (LH) proper helical arrangement of spins. The results of the present study show a good agreement with the recent theoretical study by Arima,[19] which predicts that proper helical magnetic ordering in $CuFe_{1-x}Al_xO_2$ can generate a spontaneous electric polarization along the helical axis through a variation in the metal-ligand hybridization with spin-orbit coupling.

A single crystal of $CuFe_{1-x}Al_xO_2$ with x=0.02 of nominal composition was prepared by the floating zone technique,[20]

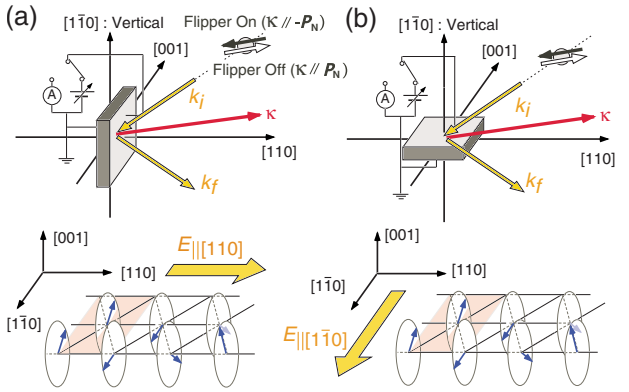

FIG. 1. (Color online) Schematic illustrations of the experimental configurations and the relationship between the direction of the poling electric field E and the proper helical magnetic structure in the FEIC phase for (a) the $E_{\|[110]}$ sample and (b) the $E_{\|[1\bar{1}0]}$ sample.

and it was cut into two pieces with disk shapes; one has the widest surface normal to the [110] axis ($E_{\|[110]}$ sample), and the other has the widest surface normal to the [1$\bar{1}$0] axis ($E_{\|[1\bar{1}0]}$ sample). The experimental configurations for these samples are illustrated in Figs. 1(a) and 1(b). Silver paste was pasted on the widest surface of each sample to make the electrodes. Polarized neutron diffraction measurements were carried out at the triple-axis neutron spectrometer (PONTA) installed by University of Tokyo at JRR-3 of the Japan Atomic Energy Agency. An incident polarized neutron with an energy of 34.05 meV was obtained by a Heusller (111) monochromator. The flipping ratio of the polarized neutron beam was ~19, and the polarization vector of the incident neutron $\boldsymbol{p}_N$ was set to be parallel or antiparallel to the scattering vector $\boldsymbol{\kappa}$ by a guide field of a Helmholtz coil and a spin flipper. The collimation was 40′-40′-40′-40′, and a pyrolytic graphite analyzer was employed. The sample was mounted in a pumped ^{4}He cryostat with a (HHL) scattering plane. In this Brief Report, we have employed a hexagonal (pseudo)basis, defined as shown in Fig. 2(a), in order to clarify the arrangements of the three magnetic domains, while a structural transition from the original trigonal structure to a monoclinic structure was reported for some of the magnetically ordered phases (including the FEIC phase) of $CuFeO_2$.[21,22] For the measurements of the spontaneous electric polarization $\boldsymbol{P}$, pyroelectric current was measured under zero electric field with increasing temperature using an electrometer (Keithley 6517A). Before each neutron diffraction or pyroelectric measurement, we performed cooling with an applied electric field from 20 to 2 K.

Before discussing the results of the present measurements, we briefly review the scattering cross section for polarized neutrons. Let us assume that a scattering system consists of RH- and LH-proper helical magnetic orderings with a propagation wave vector $\boldsymbol{q}$. According to Blume's notation,[23] the scattering cross section for a pair of magnetic satellite reflections located at $\boldsymbol{\tau}\pm\boldsymbol{q}$, where $\boldsymbol{\tau}$ is a reciprocal lattice vector, is described as follows:

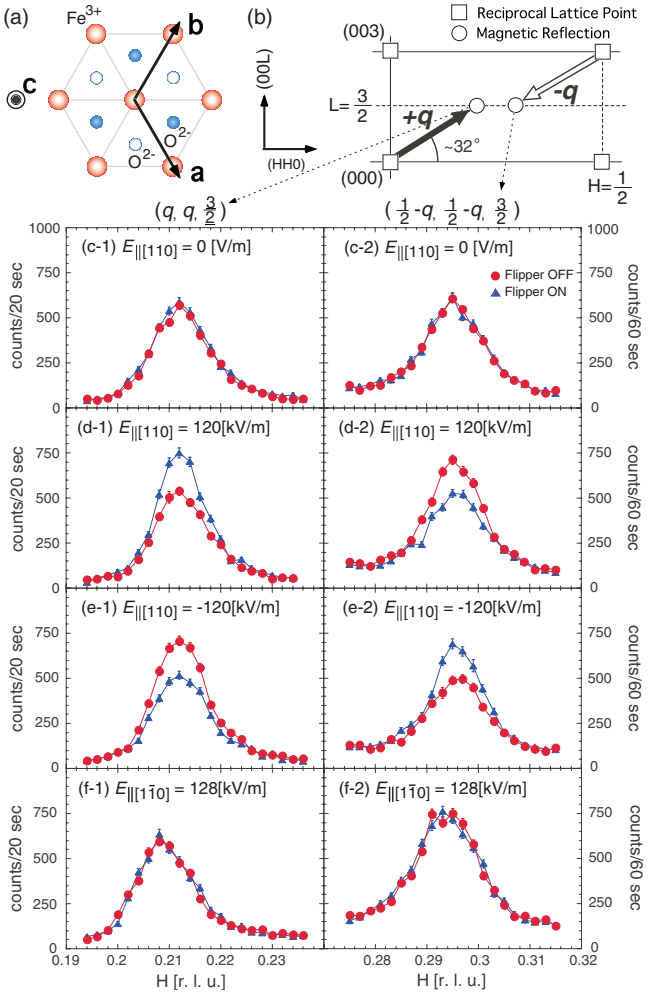

FIG. 2. (Color online) (a) The hexagonal basis represented on the Fe^{3+} triangular lattice layer. The open and filled blue circles denote O^{2-} ions located above and below the Fe^{3+} layer, respectively. (b) The location of the magnetic reflections surveyed in the present measurement in the (HHL) zone. [(c-1)–(f-2)] The diffraction profiles of $(H,H,\frac{3}{2})$ reciprocal lattice scans for the $(q,q,\frac{3}{2})$ and $(\frac{1}{2}-q,\frac{1}{2}-q,\frac{3}{2})$ magnetic Bragg reflections at T=2 K in the FEIC phase.

$$\left(\frac{d\sigma}{d\Omega}\right)_{\boldsymbol{\tau}\pm\boldsymbol{q}} \propto S(\boldsymbol{\kappa})\{[1+(\hat{\boldsymbol{e}}_z\cdot\hat{\boldsymbol{\kappa}})^2](V_{\mathrm{RH}}+V_{\mathrm{LH}}) \mp 2(\boldsymbol{p}_{\mathrm{N}}\cdot\hat{\boldsymbol{\kappa}})(\hat{\boldsymbol{e}}_z\cdot\hat{\boldsymbol{\kappa}})(V_{\mathrm{RH}}-V_{\mathrm{LH}})\}, \quad (1)$$

where $S(\boldsymbol{\kappa})$ is a factor dependent on the magnetic structure factor. Here, V_{RH} and V_{LH} are the volumes of the RH- and LH-helical orderings, respectively. $\hat{\boldsymbol{\kappa}}$ is a unit vector of the scattering vector $\boldsymbol{\kappa}$. $|\boldsymbol{p}_N|=1$. $\hat{\boldsymbol{e}}_z$ is a unit vector parallel to the helical axis. In the case of $CuFe_{1-x}Al_xO_2$, $\hat{\boldsymbol{e}}_z$ is a unit vector of [110] direction. Here, we introduce the vector spin chirality $\boldsymbol{C}$, which is defined so that $\boldsymbol{S}_i$, $\boldsymbol{S}_{i+1}$, and $\boldsymbol{C}$ in this order form a right-handed coordinate system: specifically, $\boldsymbol{C}$ is parallel (antiparallel) to the [110] direction for RH- (LH-) proper helical ordering [see Fig. 3(a)]. In the present experi-

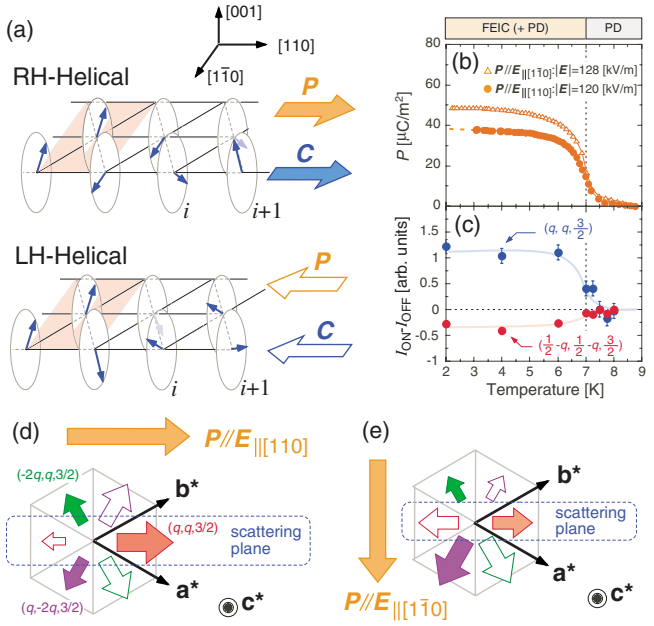

FIG. 3. (Color online) (a) The relationship between the vector spin chirality and the direction of the electric polarization. (b) The temperature variations of the electric polarization along the [110] and [1$\bar{1}$0] axes measured after cooling with a poling electric field parallel to the [110] and [1$\bar{1}$0] directions, respectively. (c) The temperature dependence of $I_{on}-I_{off}$ measured on heating after cooling with a poling electric field (120 kV/m) parallel to the [110] axis. [(d) and (e)] The schematic drawings of the distributions of the RH- (filled arrows) and LH- (open arrows) helical orderings among magnetic domains with three equivalent propagation wave vectors, $(q,q,\frac{3}{2})$, $(-2q,q,\frac{3}{2})$, and $(q,-2q,\frac{3}{2})$, when the macroscopic electric polarization emerges along (d) the [110] axis and (e) the [1$\bar{1}$0] axis. The directions of the arrows denote the (001) projection of the three modulation wave vectors. The size of the arrows shows the fractions of the RH- or LH-helical orderings.

ment, we mainly surveyed two magnetic Bragg reflections at $(q,q,\frac{3}{2})$ and $(\frac{1}{2}-q,\frac{1}{2}-q,\frac{3}{2})$. It is worth mentioning here that these reflections are assigned as $\boldsymbol{\tau}+\boldsymbol{q}$ and $\boldsymbol{\tau}-\boldsymbol{q}$ in Eq. (1), respectively, using a proper monoclinic basis.[24] From Eq. (1), the imbalance between V_{RH} and V_{LH} is written as follows:

$$\frac{V_{RH}-V_{LH}}{V_{RH}+V_{LH}}=A(\boldsymbol{\kappa})\left(\frac{I_{on}-I_{off}}{I_{on}+I_{off}}\right), \tag{2}$$

where I_{on} and I_{off} are the intensities of a magnetic Bragg reflection measured when the spin flipper is on ($\boldsymbol{p}_N \| -\boldsymbol{\kappa}$) and off ($\boldsymbol{p}_N \| \boldsymbol{\kappa}$), respectively. The values of the proportional constant $A(\boldsymbol{\kappa})$ for the $(q,q,\frac{3}{2})$ and $(\frac{1}{2}-q,\frac{1}{2}-q,\frac{3}{2})$ magnetic reflections are approximately 1 and −1, respectively.

In Fig. 2, we now show typical diffraction profiles of magnetic reflections in the FEIC phase ($T=2$ K). After cooling the $E_{\|[110]}$ sample under zero electric field, as shown in Figs. 2(c-1) and 2(c-2), there was no difference between I_{on} and I_{off} for both of the $(q,q,\frac{3}{2})$ and the $(\frac{1}{2}-q,\frac{1}{2}-q,\frac{3}{2})$ reflections. This result indicates that the fractions of the RH- and LH-helical magnetic orderings were equal to each other. After cooling the $E_{\|[110]}$ sample under a poling electric field (120 kV/m) parallel to the [110] direction, I_{on} was greater than I_{off} for the $(q,q,\frac{3}{2})$ reflection, and this relationship between I_{on} and I_{off} was reversed for the $(\frac{1}{2}-q,\frac{1}{2}-q,\frac{3}{2})$ reflection, as shown in Figs. 2(d-1) and 2(d-2). By a reversal of the direction of the poling electric field applied on cooling, this relationship between I_{on} and I_{off} for each magnetic satellite was reversed, as shown in Figs. 2(e-1) and 2(e-2). However, no imbalance between I_{on} and I_{off} was observed for the $E_{\|[1\bar{1}0]}$ sample after cooling under a poling electric field (128 kV/m) parallel to the [1$\bar{1}$0] direction, as shown in Figs. 2(f-1) and 2(f-2). These results show that a poling electric field along the [110] axis induces an imbalance between the fractions of the RH- and LH-helical orderings, but a poling electric field along the [1$\bar{1}$0] axis does not. Taking into account of the fact that a poling electric field along the [110] axis also induces macroscopic electric polarization along the [110] axis [see Fig. 3(b)], we conclude that proper helical magnetic ordering generates an electric polarization along the helical axis, and moreover, there is a one-to-one correspondence between the vector spin chirality and the direction of electric polarization, as illustrated in Fig. 3(a).

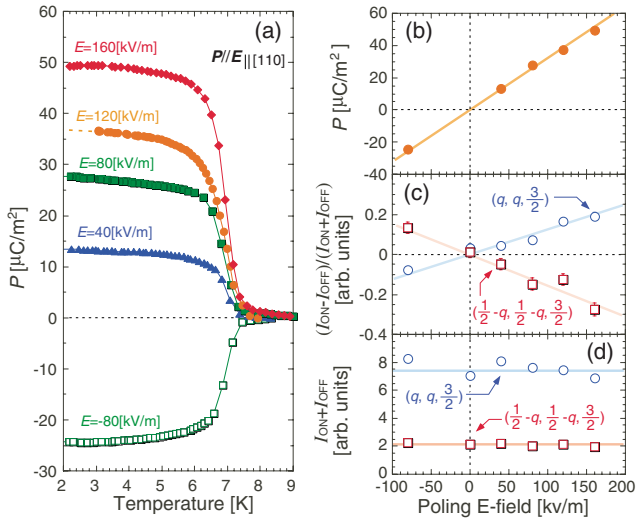

FIG. 4. (Color online) (a) Temperature variations of the electric polarization along the [110] axis measured after cooling under various poling electric fields along the [110] axis. [(b)–(d)] The poling electric field dependence of (b) the spontaneous electric polarization, (c) $(I_{on}-I_{off})/(I_{on}+I_{off})$, and (d) $(I_{on}+I_{off})$ at $T=2$ K. The colored solid lines are guides for the eyes.

A poling electric field along the [1$\bar{1}$0] axis also induces macroscopic electric polarization along the [1$\bar{1}$0] axis, as shown in Fig. 3(b). In this case, an imbalance between the fractions of the RH- and LH-helical orderings must be induced in the magnetic domains with modulation wave vectors $(q,-2q,\frac{3}{2})$ and $(-2q,q,\frac{3}{2})$, as illustrated in Fig. 3(e).

Figures 4(a)–4(c) show the poling electric field dependence of the spontaneous electric polarization and the imbalance between I_{on} and I_{off} for the $E_{\|(110)}$ sample. We found that both the magnitude of the electric polarization and the imbalance between I_{on} and I_{off} at $T=2$ K are proportional to the

poling electric field applied on cooling. In addition, the temperature variation of $I_{on}-I_{off}$, which was measured in a warming run under zero electric field after cooling with a poling electric field parallel to the [110] axis, is similar to that of the spontaneous electric polarization, as shown in Fig. 3(c). These results apparently show that the macroscopic electric polarization arises from the "imbalance" between the fractions of the RH- and LH-helical magnetic orderings. Note that the fractions of the RH- and LH-helical magnetic orderings cannot be determined accurately in the present experiments because the thermally induced partially disordered (PD) state, which has a collinear incommensurate magnetic structure with almost the same wave number as that of the FEIC magnetic ordering, is supposed to remain even in the FEIC phase owing to the pinning effect by nonmagnetic impurity ions.[11] While the imbalance between I_{on} and I_{off} apparently shows the poling electric field dependence as mentioned above, the sum of I_{on} and I_{off} does not [see Fig. 4(d)], that is, the application of a poling electric field within $|E| < \sim 160$ kV/m, does not affect the fractions of the three magnetic domains. This result implies that the fractions of the three magnetic domains are determined by the fractions of the monoclinic lattice domains, which have been already formed in the high-temperature (paraelectric) PD phase.[21,22]

In conclusion, we have established the relationship between the electric polarization vector and the magnetic modulation wave vector including the vector spin chirality in the delafossite multiferroic $CuFe_{1-x}Al_xO_2$. The present polarized neutron diffraction and pyroelectric measurements clearly demonstrate that proper helical magnetic ordering in $CuFe_{1-x}Al_xO_2$ generates a spontaneous electric polarization parallel to the vector spin chirality. This shows a good agreement with the theoretical prediction by Arima,[19] suggesting that the variation in the metal-ligand hybridization with spin-orbit coupling is relevant to the microscopic origin of the ferroelectricity in this system. It is worth mentioning that in the spiral magnetic ordering of a $RMnO_3$ system, the variation in the metal-ligand hybridization does not contribute to the uniform polarization, but it does contribute to the nonuniform polarization oscillating with a period of half the magnetic modulation.[25,26] We thus conclude that $CuFe_{1-x}Al_xO_2$ is another type of magnetic ferroelectric, which will pave the way for a design of multiferroic materials.

We are grateful to T. Arima for fruitful discussions. The neutron diffraction measurement at JRR-3 was supported by ISSP of the University of Tokyo [PACS No. 7546B (5G:PONTA)]. This work was supported by a Grant-in-Aid for Scientific Research (C) (No. 19540377) from JSPS, Japan.

*nakajima@nsmsmac4.ph.kagu.tus.ac.jp

[1] T. Kimura, T. Goto, H. Shintani, K. Ishizaka, T. Arima, and Y. Tokura, Nature (London) **426**, 55 (2003).
[2] H. Katsura, N. Nagaosa, and A. V. Balatsky, Phys. Rev. Lett. **95**, 057205 (2005).
[3] M. Mostovoy, Phys. Rev. Lett. **96**, 067601 (2006).
[4] M. Kenzelmann, A. B. Harris, S. Jonas, C. Broholm, J. Schefer, S. B. Kim, C. L. Zhang, S.-W. Cheong, O. P. Vajk, and J. W. Lynn, Phys. Rev. Lett. **95**, 087206 (2005).
[5] T. Arima, A. Tokunaga, T. Goto, H. Kimura, Y. Noda, and Y. Tokura, Phys. Rev. Lett. **96**, 097202 (2006).
[6] G. Lawes, A. B. Harris, T. Kimura, N. Rogado, R. J. Cava, A. Aharony, O. Entin-Wohlman, T. Yildrim, M. Kenzelmann, C. Broholm, and A. P. Ramirez, Phys. Rev. Lett. **95**, 087205 (2005).
[7] K. Taniguchi, N. Abe, T. Takenobu, Y. Iwasa, and T. Arima, Phys. Rev. Lett. **97**, 097203 (2006).
[8] Y. Yamasaki, S. Miyasaka, Y. Kaneko, J.-P. He, T. Arima, and Y. Tokura, Phys. Rev. Lett. **96**, 207204 (2006).
[9] Y. Yamasaki, H. Sagayama, T. Goto, M. Matsuura, K. Hirota, T. Arima, and Y. Tokura, Phys. Rev. Lett. **98**, 147204 (2007).
[10] M. Kenzelmann, G. Lawes, A. B. Harris, G. Gasparovic, C. Broholm, A. P. Ramirez, G. A. Jorge, M. Jaime, S. Park, Q. Huang, A. Ya. Shapiro, and L. A. Demianets, Phys. Rev. Lett. **98**, 267205 (2007).
[11] T. Nakajima, S. Mitsuda, S. Kanetsuki, K. Prokes, A. Podlesnyak, H. Kimura, and Y. Noda, J. Phys. Soc. Jpn. **76**, 043709 (2007).
[12] S. Mitsuda, H. Yoshizawa, N. Yaguchi, and M. Mekata, J. Phys. Soc. Jpn. **60**, 1885 (1991).
[13] S. Mitsuda, M. Mase, K. Prokes, H. Kitazawa, and H. A. Katori, J. Phys. Soc. Jpn. **69**, 3513 (2000).
[14] O. A. Petrenko, G. Balakrishnan, M. R. Lees, D. M. Paul, and A. Hoser, Phys. Rev. B **62**, 8983 (2000).
[15] T. Kimura, J. C. Lashley, and A. P. Ramirez, Phys. Rev. B **73**, 220401(R) (2006).
[16] S. Kanetsuki, S. Mitsuda, T. Nakajima, D. Anazawa, H. A. Katori, and K. Prokes, J. Phys.: Condens. Matter **19**, 145244 (2007).
[17] S. Seki, Y. Yamasaki, Y. Shiomi, S. Iguchi, Y. Onose, and Y. Tokura, Phys. Rev. B **75**, 100403(R) (2007).
[18] N. Terada, S. Mitsuda, T. Fujii, K. Soejima, I. Doi, H. A. Katori, and Y. Noda, J. Phys. Soc. Jpn. **74**, 2604 (2005).
[19] T. Arima, J. Phys. Soc. Jpn. **76**, 073702 (2007).
[20] T. R. Zhao, M. Hasegawa, and H. Takei, J. Cryst. Growth **166**, 408 (1996).
[21] N. Terada, Y. Tanaka, Y. Tabata, K. Katsumata, A. Kikkawa, and S. Mitsuda, J. Phys. Soc. Jpn. **75**, 113702 (2006).
[22] F. Ye, Y. Ren, Q. Huang, J. A. Fernandez-Baca, Pengcheng Dai, J. W. Lynn, and T. Kimura, Phys. Rev. B **73**, 220404(R) (2006).
[23] M. Blume, Phys. Rev. **130**, 1670 (1963).
[24] With the proper monoclinic basis presented in Ref. 21, these magnetic reflections can be assigned as $(0,q,\frac{1}{2})$ and $(0,1-q,\frac{1}{2})$.
[25] C. Jia, S. Onoda, N. Nagaosa, and J. H. Han, Phys. Rev. B **74**, 224444 (2006).
[26] C. Jia, S. Onoda, N. Nagaosa, and J. H. Han, Phys. Rev. B **76**, 144424 (2007).